PHYSICAL REVIEW D VOLUME 23, NUMBER 2 15 JANUARY 1981

Diagrammatic derivation of the eikonal formula for high-energy scattering in Yang-Mills theory

Hung Cheng* and John A. Dickinson*
Institute for Theoretical Physics, State University of New York at Stony Brook, Stony Brook, New York 11794

Kaare Olaussen
Institute for Theoretical Physics, University of Trondheim, N-7034 Trondheim-NTH, Norway
(Received 31 January 1979)

A new calculational scheme for unitarizing S-matrix amplitudes in the high-energy limit is applied to a Yang-Mills theory with SU(2) symmetry. The vector-meson–vector-meson elastic scattering amplitude is calculated through the tenth order in the coupling constant and the result agrees with the expansion of an eikonal formula in the impact-distance space, $S = \exp(iV)$. The potential V is an infinite-dimensional matrix whose entry for a given process is related to the sum of the lowest-order amplitudes for that process, with the exchanged vector mesons Reggeized. This result is explicitly unitary.

I. INTRODUCTION

Quantum chromodynamics (QCD) is widely regarded as the leading candidate for the description of the strong interactions. In much recent work QCD perturbation theory has been applied to deep-inelastic, large-momentum-transfer scattering processes. However, the overwhelming body of high-energy scattering occurs at small momentum transfers, and if QCD is to describe strong interactions it must accurately account for these processes as well.

Qualitatively, many physical features in the small-angle, high-energy regime are explained naturally by gauge field theories. The exchange of a particle with spin J contributes a factor s^{J-1} to the scattering amplitude (logarithmic factors of s ignored). Thus, the slow variation of the total cross section with the energy indicates that high-energy scattering is mediated by particles of spin one (vector mesons). The lowest-order elastic scattering is the one-vector-meson-exchange amplitude and is real. Thus the observed smallness of the real part of the elastic scattering amplitude suggests that the one-meson-exchange process is forbidden. This can come about if the vector meson involved carries some forbidden quantum number, such as color. There are, in addition, the approximate conservation of the helicity and the smallness of the amplitude for quantum-number exchange, both of which are qualitative features of gauge field theories.

However, to truly test QCD in this small-momentum-transfer region it is necessary to develop quantitative predictions. Toward this end we have been pursuing an extensive program of diagrammatic calculations. There are significant theoretical and technical difficulties which must be overcome. On the theoretical side, one problem is that nonperturbative effects (such as quark confinement?) which are not accounted for may be important. Another problem is that we believe the perturbation series itself is divergent. Hence it is necessary to calculate to all orders in the coupling constant and to then reexpress this infinite series in such a way as to make meaningful. Even then it is necessary to assume that the sum of the terms ignored, which individually are large, is small compared to the sum of the terms kept. On the technical side, the high-energy amplitude due to the exchange of vector mesons is always proportional to s times a power of $\ln s$. For most diagrams, this power exceeds two. Thus, the scattering amplitude from a single Feynman diagram often violates the unitary (Froissart) bound $s \ln^2 s$. Since the sum of amplitudes from all diagrams must satisfy the unitarity condition, extensive cancellations occur in the summation. Therefore, a rigorous way to obtain the asymptotic behavior of the scattering amplitude is to calculate all coefficients of $s \ln^n s$, $n = 0, 1, 2, 3, \ldots$ for all diagrams, to verify that as we sum over all diagrams, the terms larger than $s \ln^2 s$ cancel, and finally to evaluate what is left after cancellation. This is an impossible task.

Although the difficulties mentioned above exist for all gauge field theories, Abelian (QED) or non-Abelian (Yang-Mills theories), we have been able to overcome most of them for the case of QED. In QED, we have formulated a new approximation scheme for high-energy scattering.[1] A procedure was developed to generate a set of diagrams which incorporates s-channel unitarity and t-channel unitarity at every step and which treats elastic and inelastic scattering processes side by side. We calculated the leading terms of these diagrams and found that the amplitudes obtained (elastic and inelastic), though formally divergent, are analytically summed into a single eikonal formula which is explicitly unitary. It then became possible to

show, under general high-energy assumptions and without resorting to diagrams, that the S matrix in QED is of the eikonal form.[2]

Technically, the calculations in Yang-Mills theories are more difficult than those in QED. First of all, the vertex of interaction in Yang-Mills theories is complicated. Second, the Yang-Mills vector meson carried color [or isospin if the gauge group is SU(2)] and may emit other vector mesons. This contrasts with the situation in QED, where the photon is chargeless and cannot emit other photons. Consequently, all Feynman diagrams of a given perturbative order in Yang-Mills theories are related by gauge invariance, and, unlike QED, it is not possible to single out a set of diagrams for summation.

In this paper, we shall devise a scheme of diagrammatic calculation for Yang-Mills theories. This scheme is a generalization of the method of summing leading terms, and is the counterpart of the diagrammatic procedure in QED. We have not found a justification for the mathematical validity of this scheme. However, because of its close similarity with the scheme in QED, which has been justified under general assumptions, it is likely that such a justification can be made in the near future. Most gratifying, the terms we obtain from this scheme again coincide exactly with the corresponding terms of an eikonal formula.

II. SCHEME OF CALCULATION

In the design of a scheme of diagrammatic computations of amplitudes in gauge theories, the most difficult general principle to incorporate is unitarity. It is not hard to understand why. Dispersion relations are automatically incorporated into individual Feynman diagrams and crossing symmetry can be satisfied by including crossed diagrams. But the unitarity condition interrelates the amplitudes of an infinite number of Feynman diagrams. Consequently, any approximation scheme which includes one Feynman diagram must include all others related to it, if the scheme is to be unitary.

To see this in more detail, we note that the scattering matrix S and the scattering amplitude $\mathfrak{M}$ are related according to

$$S=1+i(2\pi)^4\delta^{(4)}(P_i-P_f)\frac{\mathfrak{M}}{\prod_n f_n^{1/2}}, \qquad (2.1)$$

where P_i and P_f are the total four-momenta of the initial and final states, respectively, and where

$$f_n=\begin{cases}\dfrac{E_n}{m} & \text{for a fermion with energy } E_n \text{ and mass } m,\\ 2E_n & \text{for a boson.}\end{cases}$$

The product $\prod_n f_n$ in (2.1) is over all external particles. In terms of $\mathfrak{M}$, the unitarity condition is

$$\mathrm{Im}\mathfrak{M}_{fi}=\tfrac{1}{2}\sum_n (2\pi)^4\delta^{(4)}(P_i-P_n)\frac{\mathfrak{M}^*_{fn}\mathfrak{M}_{ni}}{\prod_m f_m}, \qquad (2.2)$$

where there is a kinematic factor f_m for each particle in the intermediate state.

Because of the nonlinear nature of (2.2), past schemes of diagrammatic calculations often fail this unitarity condition badly. One such example is the scheme of summing leading logarithms. In this scheme, one calculates, in each finite perturbation order, only the largest term in the high-energy limit. In Yang-Mills theories, the leading real terms are of the order of $g^2s(g^2\ln s)^n$, $n=0,1,2,\ldots$, and the leading imaginary terms are of the order of $ig^4s(g^2\ln s)^{n-1}$. The terms which are of the same perturbative order but are smaller than the leading terms by a power of $\ln s$ or more are neglected.

In both QED (Ref. 3) and the Yang-Mills theory[4,5] it has been shown that the amplitudes in the leading-logarithm approximation violate the Froissart bound. In particular, for an SU(2) Yang-Mills theory with an isospin-$\frac{1}{2}$ Higgs doublet, Fadin, Kuraev, and Lipatov[4] and Cheng and Lo[5] have separately found that for vector-meson–vector-meson elastic scattering, $W+W\to W+W$, the sum of the leading logarithmic terms violates the Froissart bound in the $I=0$ channel (no exchange of isospin).

This violation is not unexpected even without any detailed calculation. To see this, let us replace $\mathfrak{M}$, for example, by the one-vector-meson-exchange amplitude and substitute it into the right-hand side of (2.2). What we obtain is not the imaginary part of the one-vector-meson-exchange amplitude we put in, but a new term which is equal to the imaginary part of the two-vector-meson-exchange amplitude. This means that the one-vector-exchange amplitude alone does not satisfy the unitarity condition. How about the sum of the one-vector-meson-exchange amplitude and the two-vector-meson-exchange amplitude? If we replace $\mathfrak{M}$ by this sum, the right-hand side of (2.2) is not equal to the imaginary part of this sum, but contains terms related to three-vector-meson exchange and four-vector-meson exchange. Repeating this process, we obtain an infinite set of diagrams which are related to the one-vector-exchange amplitude through the unitarity condition. In QED, the leading-logarithms approximation does not include these diagrams.

The situation is similar in Yang-Mills theories, but with an interesting modification. To be explicit, consider the Yang-Mills theory of SU(2) with

an isodoublet of Higgs mesons. The sum of the leading real terms for the elastic scattering amplitude is equal to the one-vector-meson-exchange amplitude with the exchanged meson Reggeized:

$$-\frac{2g^2 s^{\alpha(\vec{\Delta})}}{\vec{\Delta}_\perp^{\,2}+\lambda^2}\,\vec{T}^{(1)}\cdot\vec{T}^{(2)}. \tag{2.3}$$

In (2.3), g, λ, and $\vec{\Delta}_\perp$ are, respectively, the coupling constant, the vector-meson mass, and the momentum transfer, $\alpha(\vec{\Delta})$ is the Regge trajectory on which the vector meson lies:

$$\alpha(\vec{\Delta})=1-\frac{(\vec{\Delta}_\perp^{\,2}+\lambda^2)g^2}{2\pi}\times\int\frac{d^2q_\perp}{(2\pi)^2}\,\frac{1}{(\vec{q}_\perp^{\,2}+\lambda^2)[(\vec{\Delta}_\perp-\vec{q}_\perp)^2+\lambda^2]} \tag{2.4}$$

and $\vec{T}^{(1)}$ and $\vec{T}^{(2)}$ are the isospin matrices associated with the external particles. It is understood that they are inserted between the isospin wave functions of these particles. We note that, if we replace $\alpha(\vec{\Delta})$ by unity, (2.3) becomes the lowest-order amplitude of one-vector-meson exchange. The leading real terms from high-order amplitudes modify $\alpha(\vec{\Delta})$ into the expression given by (2.4). For inelastic processes, the leading real terms similarly sum into Reggeized forms of the corresponding lowest-order amplitudes.[4,6] In contrast, the photon in QED is not Reggeized.

Upon replacing $\mathfrak{M}$ by these leading real terms of Reggeized amplitudes, the right-hand side of the unitarity condition (2.2) becomes, in the high-energy limit, the leading imaginary terms calculated in Refs. 4 and 5. For the same reason as was given above, the sum of these leading real terms and leading imaginary terms does not satisfy unitarity. Consequently, this sum does not have to obey the Froissart bound.

A scheme of calculation consistent with unitarity must therefore go beyond summing leading terms. At first sight, this is a nightmarish prospect, as it is extermely difficult to calculate nonleading terms from any diagram, let alone all diagrams. It proves helpful, however, to look at the leading-logarithm terms calculated from another vantage point. We shall concentrate on the elastic scattering amplitude only. The scattering amplitude $\mathfrak{M}$ for each diagram is the product of an isospin factor I and a space-time factor M (which is independent of isospin), $\mathfrak{M}=M\cdot I$. The isospin factor I for the leading real terms is equal to $\vec{T}^{(1)}\cdot\vec{T}^{(2)}$ as given in (2.3). Let us denote the isospin of the external particles by T. (For example, $T=\frac{1}{2}$ for an isodoublet, but here we keep T arbitrary.) Then $\vec{T}^{(1)}\cdot\vec{T}^{(2)}$ is a second-order polynomial in T. The leading imaginary terms are obtained by squaring the leading real terms, and are hence fourth-order polynomials of T. The leading real terms and the leading imaginary terms can therefore be viewed as the leading terms for the coefficients of T^2 and T^4, respectively.

If we replace $\mathfrak{M}$ by a sum in the form of $c_2T^2+c_4T^4$ and substitute it into the right-hand side of the unitarity condition (2.2), which is quadratic in $\mathfrak{M}$, we obtain, in addition to a T^4 term, T^6 and T^8 terms. This is another way to see why a sum of this form cannot be unitary. This consideration further leads to a minimum requirement for a unitary result: terms of T^{2n}, $n=1,2,3,\ldots$ must be included.

Consequently, it is natural to propose the following scheme: *calculate the leading-logarithm terms for the coefficients of* T^{2n}, $n=1,2,3,\ldots$. The coefficients of $n=1$ and 3 are the traditional leading-logarithm terms for the real part and the imaginary part of the scattering amplitude. The rest of the coefficients are nonleading in the traditional sense [see (2.5) below for the order of magnitude of these terms]. Our scheme is therefore a generalization of the scheme of summing leading-logarithm terms.

What is the justification of our scheme? Mathematically, there is none. The main objection to our scheme is the same as to any scheme of diagrammatic calculation: we have neglected infinitely many terms which are larger than the Froissart bound $s\ln^2 s$. It is possible that the sum of these neglected terms entirely invalidates the result in this paper.

We believe, however, that there are merits in our scheme. This belief is based on the following two findings.

(i) While the leading terms of T^{2n}, $n=1,2,3,\ldots$ are necessary for a unitary result, it is by no means clear that they are sufficient. Let us denote the sum of the T^{2n} leading terms for the $I=0$ channel by c_n, $n=2,3,\ldots$. Then, while c_2 is large enough to violate the Froissart bound, $c_3, c_4, \ldots$, etc. are even larger, with $|c_2|\ll|c_3|\ll|c_4|\ll\cdots$ in the high-energy limit. It is, therefore, remarkable that these terms are equal to the corresponding terms of an eikonal formula, which is explicitly unitary. This has been verified up to the tenth order, passing 27 nontrivial tests on the coefficients. Such a spectacle is not likely to be accidental, but should be due to a higher wisdom we still fail to grasp.

(ii) The terms calculated in our scheme are the counterparts of the terms calculated from diagrams in QED.[7] Since the general validity of the eikonal formula in QED has been established in a nonperturbative approach, it gives us impetus to make a similar investigation in the Yang-Mills theories. For this purpose, the Reggeization of the vector meson will serve as an important clue.

Finally, there is a way to classify the terms we have calculated. The leading T^{2n} terms are of the order of

$$(Tg)^{2n}s(g^2\ln s)^m, \quad m=0,1,2,\ldots. \tag{2.5}$$

In other words, these terms can be factorized into powers of (gT) and powers of $(g^2\ln s)$, with no additional factors of g^2 left. The terms neglected are of the order of a positive power of g^2 times $(Tg)^{2n}s(g^2\ln s)^m$. We may therefore think of the terms calculated in our scheme as those which should be kept if g^2 is small, while (Tg) and $g^2\ln s$ are both of the order of unity. Although the mathematical basis of this scheme is yet unknown,[8] we emphasize that the purpose of our scheme is to derive a unitary result which may provide us with a hint of the correct answer. We may then proceed to find this answer by more rigorous methods. The variable T is merely a guide to identify the terms we must keep.

III. THE EIKONAL FORMULA

Since we shall have to present a substantial amount of calculations, which are more complicated than the final answer, it appears desirable to give the result first. We shall do this in the present section. We shall also discuss the significance of the result here.

Let us begin with a discussion of the eikonal formula of Molière.[9] Consider the scattering of a fermion by a potential $V(x,y,z)$. The scattering amplitude is obtained by solving the Dirac equation. Except for a few special cases (Coulomb potential, square-well potential, etc.), this cannot be done in a closed form. However, in the high-energy limit, a remarkable simplification takes place and it becomes possible to express the S matrix at fixed impact distances as[10]

$$S(\vec{b}_\perp) \cong e^{iV(\vec{b}_\perp)}, \tag{3.1}$$

where

$$V(\vec{b}_\perp)=\int_{-\infty}^{\infty} V(x,y,z)dz \tag{3.2}$$

with

$$\vec{b}_\perp = x\vec{e}_1 + y\vec{e}_2 .$$

In the above, the z axis is taken to be in the direction of the incident momentum. We note that, since $V(\vec{b}_\perp)$ is the lowest-order term in the scattering amplitude, (3.1) says that, in the high-energy limit, all the higher-order terms in the scattering are included by simply exponentiating the lowest-order term. The usual scattering amplitude for fixed momentum transfer is related to $S(b_\perp)$ by a Fourier transform:

$$\mathfrak{M}=2is\int d^2b\, e^{+i\vec{\Delta}_\perp\cdot\vec{b}_\perp}[1-S(\vec{b}_\perp)]. \tag{3.3}$$

In QED, particles can be created or destroyed—a phenomenon not present in potential scattering. However, it is possible to show that (3.1) still holds, where V involves creation and annihilation operators.[1,2] In particular, if we restrict ourselves to a set of diagrams generated by a unitarization scheme,[1] V is the (Hermitian) operator whose matrix elements V_{nm} are the lowest-order amplitudes for the scattering from state m to state n.

If we neglect all matrix elements of V except the one for elastic scattering, we recover Molière's result. The infinitely many terms due to pair creations and pair annihilations, most of them larger than $s\ln^2 s$, simply sum up to produce the inelastic matrix elements of V. Since V is Hermitian, e^{iV} is unitary. This is a most natural way for the infinitely many large terms to cancel.

It is tempting to conjecture that the scattering amplitude in Yang-Mills theory is also equal to e^{iV}, where the matrix elements of V are again equal to the lowest-order amplitudes for the corresponding processes. Although this exponentiation formula is unitary, it does not agree with the diagrammatic calculations. For example, this exponential formula does not generate the leading T^2 terms which Reggeize the vector meson; neither does it generate the other leading T^{2n} terms. Indeed, because of the non-Abelian nature of the isospin matrices, the leading T^{2n} terms have far fewer cancellations of the $\ln s$ factors, and are much more complicated than the corresponding terms in QED. The exponential of the lowest-order matrix elements, correct for QED, does not produce the multitude of uncanceled logarithmic terms in Yang-Mills theory. Fortunately, we find that the exponential formula works if we make a slight modification: making the matrix elements of V equal to the lowest-order amplitudes *with the exchanged mesons Reggeized*.

Before writing down the explicit form of the eikonal operator V in the Yang-Mills theory, we need some preliminaries. In the center-of-momentum system, where the total energy is $\sqrt{s}=2\omega$, $s\to\infty$, precisely two particles have energies $\sim\omega$, and any other particles have much smaller energies. Thus, the extremely energetic particles have approximately equal and opposite momenta of magnitude $\sim\omega$. Let these momenta be oriented predominantly along the z axis, and for an arbitrary four-vector $k=(k_0,k_1,k_2,k_3)$ define $k_\pm = k_0 \pm k_3$. Then one of these extremely energetic particles has plus momentum $\sim 2\omega$ and minus momentum $O(1/\omega)$, and vice versa for the other one.

At high energies, the helicities in the c.m.

system are conserved. Let ϵ_1, ϵ_2 ($\epsilon_{1'}, \epsilon_{2'}$) be the polarization vectors for the incoming (outgoing) extremely energetic particles. If the vector mesons are transversely polarized, then in each amplitude there is a factor of $(\vec{\epsilon}_{1\perp}\cdot\vec{\epsilon}_{1',\perp})(\vec{\epsilon}_{2\perp}\cdot\vec{\epsilon}_{2',\perp})$, which will hereafter be suppressed. (We will treat the case where the W mesons are transversely polarized.)

The result of calculation is that for elastic scattering through the tenth order, the scattering amplitude can be written in the eikonal forms (3.1) and (3.3), where V is an operator given by

$$(V(\vec{b}_\perp,s))_{fi}=\tfrac{1}{2}\int\frac{d^2\Delta_\perp}{(2\pi)^2}\,e^{-i\Delta_\perp\cdot\vec{b}_\perp}\,\frac{(\bar{\mathfrak{M}}(s,\vec{\Delta}_\perp))_{fi}}{\left(\prod_n f_n\right)^{1/2}}, \tag{3.4}$$

where the matrix elements of $\bar{\mathfrak{M}}$ for a given process are given by the sum of the lowest-order amplitudes for that process, with the propagators of the exchanged vector mesons Reggeized. For example, the matrix element of $\bar{\mathfrak{M}}$ for elastic scattering is given by (2.3). Before giving the matrix elements of $\bar{\mathfrak{M}}$ for inelastic processes, we note that the dominant contribution to the elastic scattering amplitude $\mathfrak{M}$ in (3.3) comes from those intermediate states in which the plus (or minus) momenta of all particles are far apart. Therefore, we need only consider the $\bar{\mathfrak{M}}$ matrix elements between such states. As an example of an inelastic matrix element, consider scattering from a state of three particles to a state of three particles. Let $\vec{k}_1$ and $\vec{k}_2$ be the momenta of the created and annihilated particles, respectively, and let $\vec{p}_1$ and $\vec{p}_2$ ($\vec{p}_{1'}$ and $\vec{p}_{2'}$) be the momenta of the incoming (outgoing) extremely energetic particles with large plus momentum and large minus momentum, respectively. [These states are normalized so that $\langle\vec{k}|\vec{k}'\rangle = (2\pi)^3\delta^{(3)}(\vec{k}-\vec{k}')$.] The $\bar{\mathfrak{M}}$ matrix element for that process in which $k_{1-}\ll k_{2-}$ is represented schematically in Fig. 1 and equals (suppressing isospin and polarization indices of the external particles)

$$\langle\vec{p}_{1'},\vec{p}_{2'},\vec{k}_1|\bar{\mathfrak{M}}|\vec{p}_1,\vec{p}_2,\vec{k}_2\rangle = 2g^2 s\sum_{a=1}^{3}\sum_{b=1}^{3}\sum_{c=1}^{3}\left(\frac{s_1^{\alpha(\vec{\Delta}_1)-1}}{\vec{\Delta}_{1\perp}^{\,2}+\lambda^2}\right) gV_{ab}(\Delta_1,\Delta_2,k_1)$$
$$\times\left(\frac{s_2^{\alpha(\vec{\Delta}_2)-1}}{\vec{\Delta}_{2\perp}^{\,2}+\lambda^2}\right) gV_{bc}(\Delta_2,\Delta_3,k_2)\left(\frac{s_3^{\alpha(\vec{\Delta}_3)-1}}{\vec{\Delta}_{3\perp}^{\,2}+\lambda^2}\right)(-T_a^{(1)}T_c^{(2)}). \tag{3.5}$$

In the above equation λ is the mass of the vector meson;

$$\Delta_1 = p_1 - p_{1'}, \tag{3.6a}$$

$$\Delta_2 = \Delta_1 - k_1, \tag{3.6b}$$

$$\Delta_3 = \Delta_2 + k_2 = p_{2'} - p_2, \tag{3.6c}$$

$$s_1 = (p_{1'}+k_1)^2 \sim \omega k_{1-}, \tag{3.7a}$$

$$s_2 = (k_1+k_2)^2 \sim k_{1+}k_{2-}, \tag{3.7b}$$

and

$$s_3 = (k_2+p_{2'})^2 \sim \omega k_{2+} \tag{3.7c}$$

are the squares of the energies of various pairs of particles in their respective c.m. systems; $\alpha(\vec{\Delta})$ is given by (2.4); and

$$V_{ab}(\Delta_1,\Delta_2,k)=\begin{cases} i\epsilon_{abc}\,\Gamma(\Delta_1,\Delta_2)\cdot\epsilon(k) = i\epsilon_{abc}\left[\vec{\epsilon}_\perp\cdot(\vec{\Delta}_{1\perp}+\vec{\Delta}_{2\perp}) - \epsilon_+ k_-\left(\frac{1}{2}-\frac{\vec{\Delta}_{2\perp}^{\,2}+\lambda^2}{\vec{k}_\perp^{\,2}+\lambda^2}\right)\right. \\ \qquad\left. +\epsilon_- k_+\left(\frac{1}{2}-\frac{\vec{\Delta}_{1\perp}^{\,2}+\lambda^2}{k_\perp^{\,2}+\lambda^2}\right)\right] \text{ if a vector meson with isospin } c \text{ is created,} \qquad (3.8a) \\ i\epsilon_{acb}\,\Gamma(\Delta_1,\Delta_2)\cdot\epsilon(k) = i\epsilon_{acb}\left[-\vec{\epsilon}_\perp\cdot(\vec{\Delta}_{1\perp}+\vec{\Delta}_{2\perp}) - \epsilon_+ k_-\left(\frac{1}{2}-\frac{\vec{\Delta}_{2\perp}^{\,2}+\lambda^2}{\vec{k}_\perp^{\,2}+\lambda^2}\right)\right. \\ \qquad\left. +\epsilon_- k_+\left(\frac{1}{2}-\frac{\vec{\Delta}_{1\perp}^{\,2}+\lambda^2}{\vec{k}_\perp^{\,2}+\lambda^2}\right)\right] \text{ if a vector meson with isospin } c \text{ is annihilated,} \qquad (3.8b) \\ -\lambda\delta_{ab} \text{ for a scalar } Z. \qquad (3.8c) \end{cases}$$

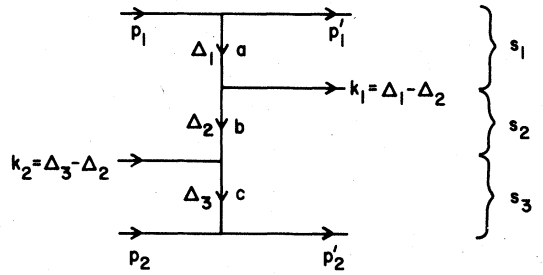

FIG. 1. A schematic representation of a matrix element of $\mathfrak{M}$. Both the space-time and isospin factors associated with this amplitude can be represented diagrammatically by precisely this diagram.

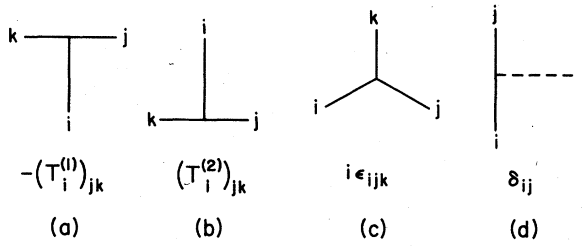

FIG. 2. The isospin factor associated with each vertex. (a) Vertex on the top high-energy line, (b) vertex on the bottom high-energy line, (c) internal three vector-meson vertex, (d) internal vector-meson–scalar vertex.

For a created or annihilated vector meson, $\epsilon(k)$ is one of the three polarization vectors such that $\epsilon(k)\cdot k=0$, $\epsilon^2(k)=-1$. $T^{(1)}$ and $T^{(2)}$ in (3.5) are the isospin matrices associated with the top and bottom high-energy lines, respectively. The isospin factor for this amplitude is the same as the isospin factor of a tree diagram with all external particles represented by horizontal lines ordered vertically according to their minus momenta and all exchanged mesons represented by vertical lines. An example is given in Fig. 1. The form of the vertex (3.8) is based on the calculation of the two-body to three-body scattering amplitude.[4,6] Note that $\Gamma\cdot k=0$. Equation (3.5) also gives the matrix element of $\mathfrak{M}$ when any number of intermediate energy particles pass through without interacting. The $\mathfrak{M}$ matrix element for any other inelastic processes in which the plus (or minus) momenta of all particles are widely separated is found by generalizing (3.5) by including the appropriate number of Reggeized propagators and vertex factors.

Because of the Reggeization of the vector meson, each V_{nm} goes to zero as we fix n and m and let s go to infinity. This does not necessarily mean, however, that the scattering amplitude $\mathfrak{M}$ goes to zero. This is because the matrix elements of $\exp(iV)$ are not simply related to those of V. For example, if we expand the exponential, the V^2 term is

$$V_{fi}^{\,2}=\sum_n V_{fn}V_{ni}\,, \tag{3.9}$$

where the sum is over a complete set of states. The smallness of each term on the right-hand side of (3.9) is compensated for by the large number of terms, i.e., the large number of intermediate states. In fact, the V^2 term corresponds to the imaginary part of the leading-logarithm approximation which we know violates the Froissart bound—thus the sum in (3.9) is very large.

In Sec. IV of this paper we outline the diagrammatic verification of the eikonal formula. We conclude in Sec. V with a discussion of the advantages, domain of validity, and generalizations of the eikonal formula in Yang-Mills theory and also compare its physical significance with that of the eikonal formula found in QED.

IV. VERIFICATION OF EIKONALIZATION

The calculation via Feynman rules had previously been done through the tenth order in the coupling constant[5]—but only in the traditional leading-logarithm approximation, which corresponds to the real T^2 and imaginary T^4 terms of our new scheme. We have now calculated the T^6, T^8, and T^{10} terms up to the tenth order.

We will discuss the diagrammatic calculation through the fourth order in some detail. We also discuss the new techniques necessary in the higher-order calculations. The results of the calculation by Feynman diagrams are given in Table II and further details of the calculation are relegated to Appendix B. For a fuller discussion, see Refs. 11 and 12.

A. Isospin calculation

The isospin factors will be calculated diagrammatically.[13] This procedure has the advantages of (i) easy comparison with the eikonal results, (ii) not having to separately check the $I=0,1,2,\ldots$ channels of isospin exchange, and, most important, (iii) being generalizable to other gauge groups, since most of the manipulations of the isospin diagrams involve the identity illustrated in Fig. 4, which is valid for all such groups.

The isospin factor associated with each Feynman diagram can be represented by precisely that diagram. Each line then carries an isospin index and the indices corresponding to all internal lines are summed over, from one to three. Each external line also has an isospin wave function, denoted χ. And each vertex has a numerical factor associated with it, as shown in Fig. 2. There, T_i are the isospin matrices which satisfy the

commutation rule

$$[T_i, T_j] = i\epsilon_{ijk} T_k , \tag{4.1}$$

and where

$$(T_i T_i)_{jk} = T(T+1)\delta_{jk} . \tag{4.2}$$

In Eqs. (4.1) and (4.2) and in the sequel a sum (from one to three) over repeated indices is assumed. If $T=1$, $(T_i)_{jk} = -i\epsilon_{ijk}$. Then the assignments given in Figs. 2(a)–2(c) are all consistent.

As an example, the isospin factor corresponding to the diagram in Fig. 3 is

$$-(\chi_1^\dagger T_i^{(1)} \chi_1)(\chi_2^\dagger T_i^{(2)} \chi_2) , \tag{4.3}$$

and is, of course, $O(T^2)$.

The diagrammatic expression of Eq. (4.1) is given in Fig. 4. Another useful identity, derived from (4.1), is

$$\begin{aligned} i\epsilon_{ijk} T_i T_j &= \tfrac{1}{2} i\epsilon_{ijk}(T_i T_j - T_j T_i) \\ &= \tfrac{1}{2} i\epsilon_{ijk}(i\epsilon_{ijl} T_l) = -T_K . \end{aligned} \tag{4.4}$$

This is expressed diagrammatically in Fig. 5 and is called the triangle contraction. [For SU(n), there is a factor $n/2$ multiplying the right-hand side of Fig. 5.] Both of the identities in Figs. 4 and 5 can be turned upside down and remain valid.

B. Second- and fourth-order calculations

One second-order Feynman diagram contributes when the high-energy particles are transversely polarized. It is shown in Fig. 3 (which is also a diagrammatic representation of its isospin factor). Its space-time amplitude is

$$2sg^2 \frac{1}{\vec{\Delta}_\perp^{\,2} + \lambda^2} . \tag{4.5}$$

The two fourth-order Feynman diagrams which contribute are shown in Figs. 6(a) and 6(b). Call their space-time amplitudes M_a and M_b, respectively. Using the isospin identities of Figs. 4 and 5, we may express the isospin factor of the diagram shown in Fig. 6(b) in terms of the isospin factors of Figs. 3 and 6(a). This is illustrated in Fig. 7. This identity exemplifies the general procedure to be used in this calculation. All isospin factors will be represented as linear combinations

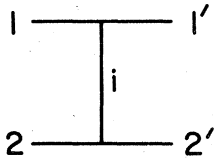

FIG. 3. A diagram whose isospin factor is given by (4.3). Equivalently, this may be considered as a diagrammatic representation of this isospin factor.

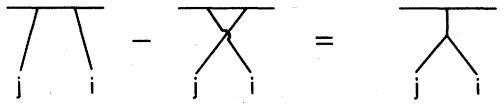

FIG. 4. The diagrammatic representation of the commutation rule (4.1).

of isospin factors whose corresponding diagrams have only vertical and horizontal lines; for purposes of future identification these isospin factors will be called "box" factors. [For example, the diagrams in Figs. 3 and 6(a) are box factors, whereas the diagram in Fig. 6(b) is not.] The advantage in this procedure is that the isospin factors generated from the exponential formula are all box factors and so the result of the Feynman-diagram calculation can be easily compared with the result from exponentiation. Furthermore, the box factor with a total of $2n$ vertices on the top and the bottom lines (which carry isospin T) is of the order of T^{2n}. Thus, the leading T^{2n} terms are easily obtained from the leading coefficients of the box factors. Now the sum of the fourth-order amplitudes equals

$$\begin{aligned} &(M_a + M_b) \times [\text{the isospin factor represented by Fig. 6(a)}] \\ &\quad - M_b \times (\text{the isospin factor represented by Fig. 3}). \end{aligned} \tag{4.6}$$

From the leading-logarithm calculation[5,14]

$$M_b \sim 2g^2 s \frac{g^2 \ln s}{2\pi} K_1 \tag{4.7}$$

and

$$M_a + M_b \sim ig^4 s K_1 , \tag{4.8}$$

where

$$K_1 = \int \frac{d^2\vec{q}_\perp}{(2\pi)^2} \frac{1}{(\vec{q}_\perp^{\,2} + \lambda^2)[(\vec{\Delta}_\perp - \vec{q}_\perp)^2 + \lambda^2]} . \tag{4.9}$$

The integral K_1 can be represented diagrammatically by a transverse-momentum diagram; see Appendix A for details. Note that the T^2 terms in (4.5) and (4.7) are real whereas the T^4 term in (4.8) is imaginary and contains no real terms proportional to s.

It is interesting to compare the fourth-order re-

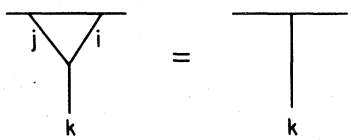

FIG. 5. The diagrammatic representation of the isospin identity given in (4.4).

FIG. 6. The fourth-order Feynman diagrams which contribute to the high-energy limit.

sults of Yang-Mills theory and QED. There are two terms in (4.6), the first one is proportional to T^4 while the second one is proportional to $T^2 \ln s$. We will see below that the $\ln s$ term in Yang-Mills theory contributes to the Reggeization of the vector meson, and is part of the potential V, whereas the first term in (4.6) contributes to the V^2 term. In contrast, because QED is Abelian, the $\ln s$ terms in QED cancel, and the fourth-order amplitude in QED contributes only to the V^2 term.

C. New techniques in higher-order calculations

In this subsection we shall discuss the new techniques in evaluating higher-order diagrams. Each of the Feynman amplitudes is equal to an isospin factor multiplied by a space-time factor. We first express the isospin factors of all Feynman diagrams which contribute in the high-energy limit in terms of the "box" factors. This is done by utilizing the commutation relation (4.1) and the triangle contraction (4.4). (For the 20 contributing sixth-order Feynman diagrams this is done in Table I.) Then we can rewrite the sum of the Feynman amplitudes for a given order as a sum of box factors each multiplied by a linear combination of space-time factors. Finally, we calculate the leading logarithmic term for each of these combinations.

The last step requires some elaboration. The leading logarithmic term of a space-time factor is best evaluated by the infinite-momentum technique. This involves expressing a propagator in the form of

$$(p_i^2 - m_i^2 + i\epsilon)^{-1} = (p_{i+} p_{i-} - \vec{p}_{i\perp}^{\,2} - m_i^2 + i\epsilon)^{-1},$$

and carrying out all integrations of the plus and the minus components of all loop momenta explicitly. These integrations give rise to logarithmic factors of s, the coefficients of which are integrals of the transverse components of all loop momenta. All this is standard except in one aspect. Here we must evaluate *combinations* of space-time factors corresponding to different Feynman diagrams. It

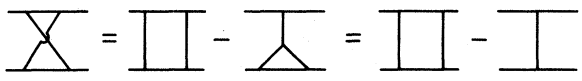

FIG. 7. An isospin identity, expressed diagrammatically.

TABLE I. In the left-most column are the 20 contributing sixth-order Feynman diagrams (or equivalently, their corresponding isospin diagrams). The isospin factors are expressed as linear combinations of the box-isospin factors with coefficients given above. The first box-isospin factor represents the T^2 terms, the next two represent the T^4 terms, and the last represents the T^6 terms. [Diagrams 5a and 5b (6a and 6b) are topologically equivalent but are distinguished by the fact that the top and bottom horizontal lines always carry very high energies.]

Feynman diagrams \ Isospin factors				
1	0	0	1	0
2	-1	0	1	0
3	0	1	0	0
4	-1	1	0	0
5a, 5b, 6a, 6b	0	1	-1	0
7, 8, 9, 10	0	1	0	0
11, 12, 13, 14	-1	1	0	0
15	0	0	0	1
16	1	-3	1	1
17, 18	0	-1	0	1
19, 20	0	-2	1	1

proves helpful to rewrite each combination into sums of subcombinations. Each subcombination includes the contribution of only the Feynman diagrams which differ by a permutation of the order in which exchanged vector mesons are attached to the top (or bottom) horizontal lines, each weighted by a number coming from the box isospin factors. It therefore facilitates the calculation if we first perform the summation over the products of such factors. There is an approximation which we can make for the propagators on the top (or bottom) lines. This approximation is based on the fact that, for the leading term, almost all of the incident plus (minus) momentum 2ω flows through the top (bottom) horizontal line. Thus, referring to Fig. 8(a), we may write, for example,

$$(p_1 + q_1)^2 - m^2 \sim 2\omega q_{1-},$$

$$(p_1 + q_1 + q_2)^2 - m^2 \sim 2\omega(q_{1-} + q_{2-}),$$

etc.

Thus the product of propagators on the top lines of the diagrams in Fig. 8(a) is proportional to

$$\frac{1}{(q_{1-}+i\epsilon)}\,\frac{1}{(q_{1-}+q_{2-}+i\epsilon)}\,\frac{1}{(q_{1-}+q_{2-}+q_{3-}+i\epsilon)}\,.$$

The simplest example of summation occurs when we sum over all the permutations of the order of the exchanged vector mesons with all weighting numbers equal.[15] In this case we wish to evaluate

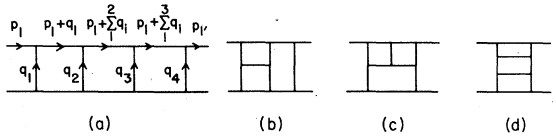

FIG. 8. Examples of the four classes of eighth-order diagrams which contribute convergent transverse-momentum integrations.

$$\delta\Big(\sum_{i=1}^{n} q_i\Big)\sum_{\sigma}\frac{1}{(q_{\sigma(1)}+i\epsilon)}\,\frac{1}{(q_{\sigma(1)}+q_{\sigma(2)}+i\epsilon)}\cdots\frac{1}{\Big(\sum_{i=1}^{n-1} q_{\sigma(i)}+i\epsilon\Big)}\,, \tag{4.10}$$

where σ is the permutation of the integers $\{1,2,\ldots,n\}$ which takes i into $\sigma(i)$, the sum in (4.10) is over all $n!$ permutations, and q is an abbreviation of q_{-}. Consider the Fourier transform of a single term in (4.10):

$$\int\prod_{i=1}^{n} dq_i \prod_{i=1}^{n} e^{-ix_i q_i}\,\delta\Big(\sum_{i=1}^{n} q_i\Big)\frac{1}{q_1+i\epsilon}\,\frac{1}{q_1+q_2+i\epsilon}\cdots\frac{1}{q_1+q_2+\cdots+q_{n-1}+i\epsilon}$$

$$=\int\prod_{i=1}^{n-1} dq_i \prod_{i=1}^{n-1} e^{-i(x_i-x_n)q_i}\,\frac{1}{q_1+i\epsilon}\,\frac{1}{q_1+q_2+i\epsilon}\cdots\frac{1}{q_1+q_2+\cdots q_{n-1}+i\epsilon}\,. \tag{4.11}$$

If $x_n > x_{n-1}$ the contour may be closed in the upper half of the complex q_{n-1} plane to give zero; and if $x_{n-1} > x_n$, by closing in the lower-half-plane, (4.11) equals

$$(-2\pi i)\int\prod_{i=1}^{n-2} dq_i \prod_{i=1}^{n-2} e^{-i(x_i-x_{n-1})q_i}\,\frac{1}{q_1+i\epsilon}\,\frac{1}{q_1+q_2+i\epsilon}\cdots\frac{1}{q_1+q_2+\cdots+q_{n-2}+i\epsilon}\,. \tag{4.12}$$

Continuing in this manner we find that (4.11) equals

$$\begin{aligned}&(-2\pi i)^n \quad \text{if } x_1>x_2>\cdots>x_{n-1}>x_n\,,\\ &0 \quad \text{otherwise}\,.\end{aligned} \tag{4.13}$$

Therefore, summing over all permutations,

$$\int\prod_{i=1}^{n} dq_i \prod_{i=1}^{n} e^{-ix_i q_i}\delta\Big(\sum_{i=1}^{n} q_i\Big)\sum_{\sigma}\frac{1}{q_{\sigma(1)}+i\epsilon}\cdots\frac{1}{\sum_{i=1}^{n-1} q_{\sigma(i)}+i\epsilon}=(-2\pi i)^{n-1} \tag{4.14}$$

and taking the inverse Fourier transform, (4.10) equals

$$(-2\pi i)^{n-1}\prod_{i=1}^{n}\delta(q_i)\,. \tag{4.15}$$

We give another example from the sixth-order calculations. From the third column of Table I, one of the subcombinations involves diagrams 16, 19, and 20. When we calculate this subcombination, we need to evaluate

$$\delta\Big(\sum_{i=1}^{3} q_i\Big)\Big(\frac{1}{(q_3+i\epsilon)(q_3+q_2+i\epsilon)}+\frac{1}{(q_3+i\epsilon)(q_3+q_1+i\epsilon)}+\frac{1}{(q_2+i\epsilon)(q_2+q_3+i\epsilon)}\Big)\,. \tag{4.16}$$

If we define

$$(x_1x_2\cdots x_n)=\begin{cases}1 & \text{if } x_1>x_2>\cdots>x_n\,,\\ 0 & \text{otherwise}\,,\end{cases} \tag{4.17}$$

then the Fourier transform of (4.16) is

$$(-2\pi i)^2((321)+(312)+(231))=(-2\pi i)^2(31)\,, \tag{4.18}$$

and the inverse transform of (4.18) is

$$(-2\pi i)^2\int\frac{dx_1}{2\pi}\,\frac{dx_2}{2\pi}\,\frac{dx_3}{2\pi}\,e^{ix_1q_1+ix_2q_2+ix_3q_3}$$

$$=(-2\pi i)\,\frac{1}{q_3+i\epsilon}\,\delta(q_3+q_1)\delta(q_2)\,. \tag{4.19}$$

This illustrates the general idea: transform to

x space, simplify, and transform back to q space. This method can be applied even if the nonzero weighting factors are different, which happens in our calculations.

D. Higher-order calculations

The sixth-order diagrams contain six vertices and hence do not contribute to T^8, T^{10},... terms. In fact, only the three-meson-exchange diagrams (diagrams 15–20 in Table I) contribute to the T^6 terms (they also contribute to the T^4 terms). The rest of the diagrams in Table I contribute to the T^4 and T^2 terms.

The details of calculations can be found in Appendix B and we shall discuss only the results here. The sum of the T^2 terms of the second through sixth orders are equal to the first three terms in the power-series expansion of

$$2g^2 s \frac{1}{\vec{\Delta}_\perp^2+\lambda^2} s^{-g^2(\Delta_\perp^2+\lambda^2)(1/2\pi)K_1} \times(\text{the isospin factor of Fig. 3}). \quad (4.20)$$

This indicates that the vector meson Reggeizes. The remaining terms, while complicated, simply produce the sixth-order terms in the Reggeized V^2 and V^3 terms in e^{iV}. In particular, the sums of V and V^3 terms are real, and the sum of V^2 terms is imaginary. All divergent transverse-momentum integrals cancel upon summation.

For the eighth and the tenth order, we assume that the divergent transverse-momentum integrals also cancel upon summation. (See, however, Ref. 5 for the cancellation of divergent integrals of T^2 and T^4, up to the eighth order.) In the eighth order, there are four classes of diagrams which contribute convergent transverse-momentum integrals. Examples are shown in Fig. 8. All other diagrams of these four classes can be obtained by up-down inversion, by replacing a horizontal vector-meson line by a scalar or by a four-vertex, by rearranging the order in which the mesons attach to the high-energy lines, or by any combination of these processes.

Diagrams of the class exemplified by the diagram in Fig. 8(a) contribute to the T^8, T^6, and T^4 terms. Diagrams such as that in Fig. 8(b) contribute to the T^6 and T^4 terms. Diagrams such as that in Fig. 8(c) contribute to the T^4 terms. Diagrams such as that in Fig. 8(d) contribute to the T^4 and T^2 terms.

Similar classifications can be made for the tenth-order diagrams. The results of the eighth-order calculations are given in Table II. The tenth-order results are given in Refs. 5 and 16.

TABLE II. A summary of the Feynman-diagram calculation through the eighth order. The amplitudes on the right-hand side come from the prototype Feynman diagram and all others related to it by up-down inversion, by replacing a vector meson by a scalar or by a four-vertex, or by any combination of the processes. These amplitudes are written in terms of transverse-momentum diagrams and isospin diagrams.

Prototype Feynman Diagrams	Scattering Amplitude $\mathfrak{M}$
	$2g^2 s \frac{1}{\vec{\Delta}_\perp^2+\lambda^2}$ 
	$ig^4 s$  $-2g^2 s\left(\frac{g^2 \ln s}{2\pi}\right)$ 
	$-ig^4 s\left(\frac{g^2 \ln s}{2\pi}\right)$  $+\frac{1}{2}ig^4 s\left(\frac{g^2 \ln s}{2\pi}\right)\lambda^2$  $+g^2 s\left(\frac{g^2 \ln s}{2\pi}\right)^2$ 
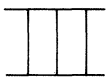	$-\frac{1}{3}g^6 s$ $+2ig^4 s\left(\frac{g^2 \ln s}{2\pi}\right)$ 
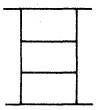	$\frac{1}{8}ig^4 s\left(\frac{g^2 \ln s}{2\pi}\right)^2$  $-\frac{1}{4}ig^4 s\left(\frac{g^2 \ln s}{2\pi}\right)^2$  $+\frac{1}{8}ig^4 s\left(\frac{g^2 \ln s}{2\pi}\right)^2 \lambda^4$  $-\frac{1}{3}g^2 s\left(\frac{g^2 \ln s}{2\pi}\right)^3$ 
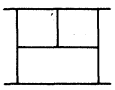	$-ig^4 s\left(\frac{g^2 \ln s}{2\pi}\right)^2$  $+2ig^4 s\left(\frac{g^2 \ln s}{2\pi}\right)^2$  $-ig^4 s\left(\frac{g^2 \ln s}{2\pi}\right)^2 \lambda^2$ 
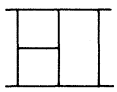	$\frac{1}{3}g^6 s\left(\frac{g^2 \ln s}{2\pi}\right)$  $-\frac{1}{2}g^6 s\left(\frac{g^2 \ln s}{2\pi}\right)\lambda^2$  $+ig^4 s\left(\frac{g^2 \ln s}{2\pi}\right)^2$ 
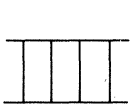	$-\frac{1}{12}ig^8 s$  $-\frac{2}{3}g^6 s\left(\frac{g^2 \ln s}{2\pi}\right)$  $+g^6 s\left(\frac{g^2 \ln s}{2\pi}\right)$  $ig^4 s\left(\frac{g^2 \ln s}{2\pi}\right)^2$

E. Calculation from the eikonal formula

The high-energy elastic scattering amplitude $\mathfrak{M}$ is the sum of infinitely many terms coming from infinitely many Feynman diagrams. We believe that the summation of the leading T^{2n} terms can be performed and the result expressed in closed form. To demonstrate that this is so through the

TABLE III. The results, through the tenth order, of the calculation from the eikonal formula. On the left-hand side are the eikonal diagrams which generate the V, V^2, . . . , V^5 terms in the expansion of the eikonal formula. The degree of Reggeization is indicated by multiple lines. On the right-hand side are the amplitudes which come from the indicated eikonal diagrams and all others related to them by rearranging the order of the factors or by up-down inversion. These amplitudes are written in terms of transverse-momentum diagrams and isospin diagrams.

Eikonal Diagram	Scattering Amplitude $\mathfrak{M}$
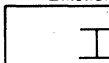	$2g^2 s \frac{1}{\Delta_\perp^2+\lambda^2}$ I
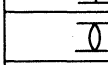	$-2g^2 s \frac{g^2 I n s}{2\pi}$ I
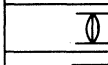	$g^2 s \left(\frac{g^2 I n s}{2\pi}\right)^2$ I
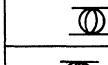	$-\frac{1}{3} g^2 s \left(\frac{g^2 I n s}{2\pi}\right)^3$ I
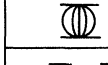	$\frac{1}{12} g^2 s \left(\frac{g^2 I n s}{2\pi}\right)^4$ I
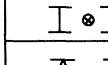	$ig^4 s$ II
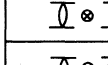	$-2ig^4 s \frac{g^2 I n s}{2\pi}$ II
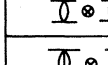	$ig^4 s \left(\frac{g^2 I n s}{2\pi}\right)^2$ II
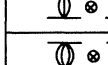	$ig^4 s \left(\frac{g^2 I n s}{2\pi}\right)^2$ II
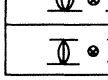	$-\frac{1}{3} ig^4 s \left(\frac{g^2 I n s}{2\pi}\right)^3$ II
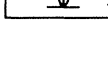	$-ig^4 s \left(\frac{g^2 I n s}{2\pi}\right)^3$ II

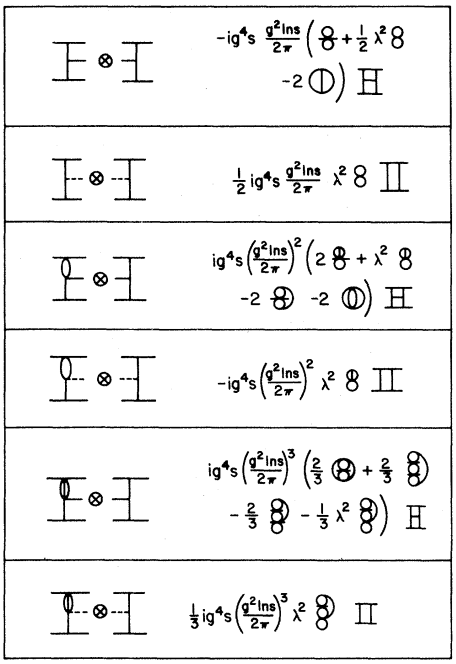

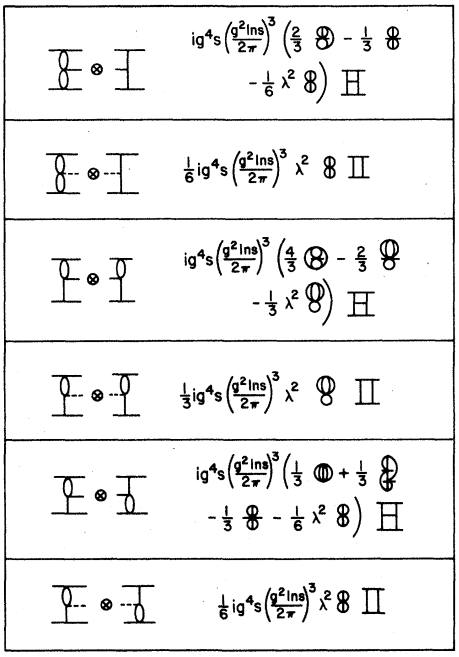

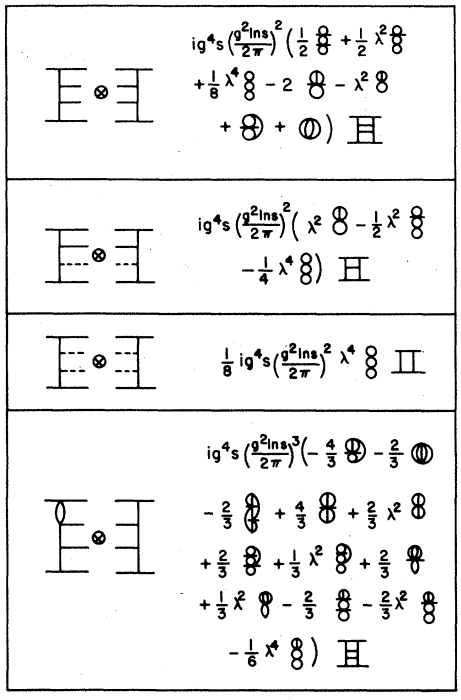

TABLE III. (*Continued*)

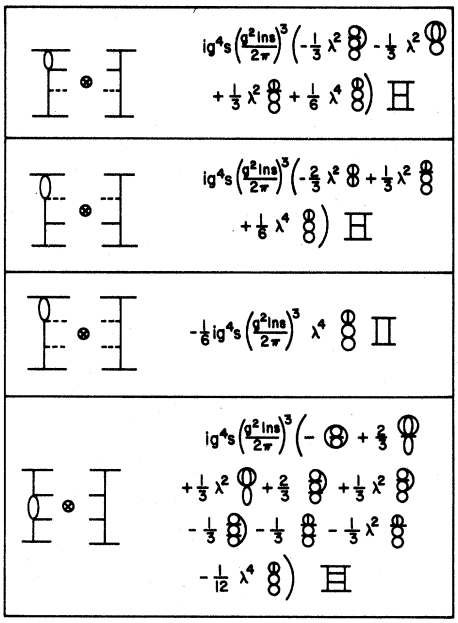

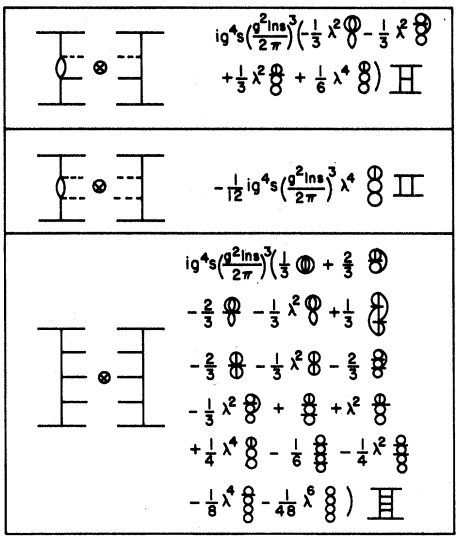

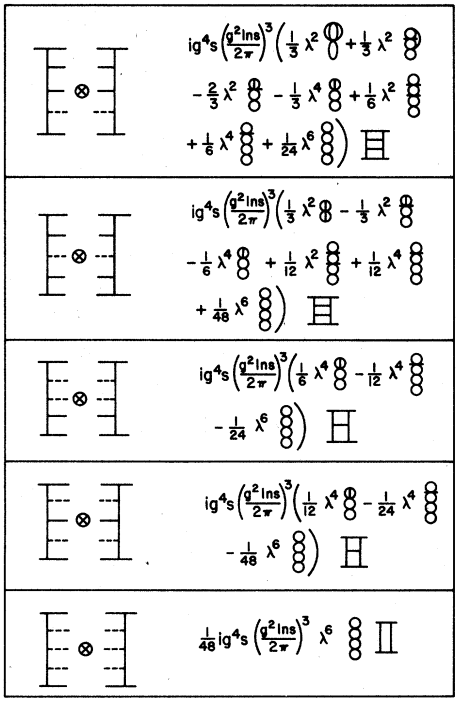

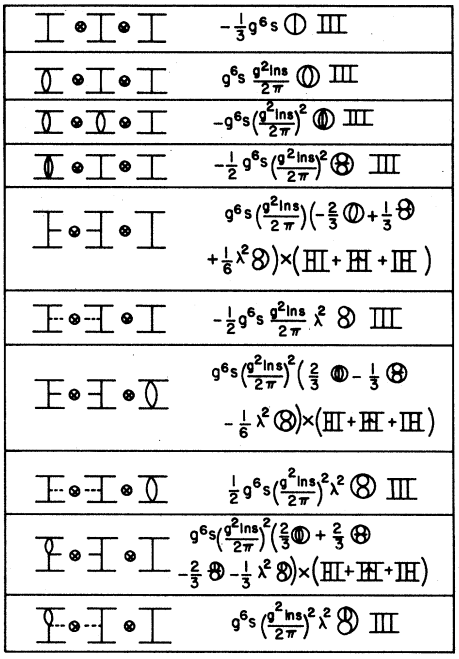

TABLE III. (*Continued*)

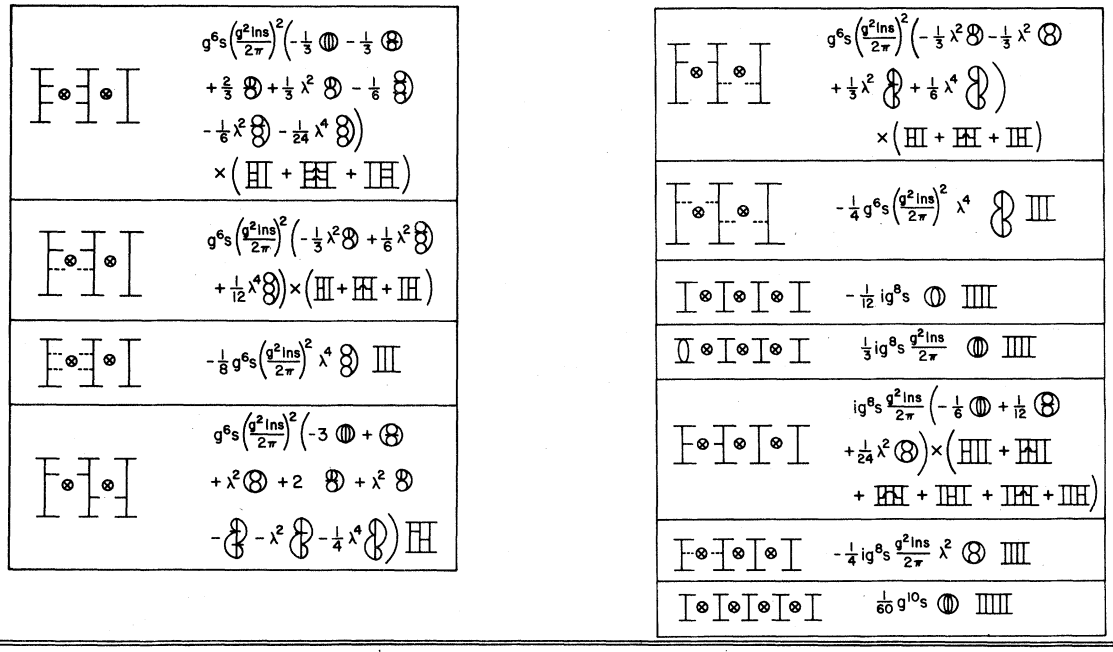

tenth order, we have shown that the $(Tg)^n(g^2\ln s)^m$ terms from the Feynman-diagram calculation agree with the corresponding terms of the eikonal formulas (3.1) and (3.3).

The techniques of the calculation from exponentiation are discussed in Appendix C. The results up to the tenth order are given in Table III.

V. CONCLUSIONS

There are two major advantages of the eikonal form. First, it is explicitly unitary. Second, it expresses the scattering amplitude in closed form. This is important because we believe that the perturbation series is itself divergent. In Appendix D we give an example of a model in one space and one time dimensional in which the infinite series

$$\exp(iV)=\sum_{n=0}^{\infty}\frac{(iV)^n}{n!} \tag{5.1}$$

does diverge. This illustrates the danger in dealing with only a finite number of terms in the expansion (5.1). But if the perturbation series is divergent, what is the meaning of the eikonal form? Consider a complete set of orthonormal eigenfunctions $\{|\mu\rangle\}$ of the potential V,

$$\langle\mu|V|\nu\rangle=V_\mu\delta_{\mu\nu}. \tag{5.2}$$

If we expand each matrix element in terms of these eigenfunctions, then

$$\langle f|e^{iV}|i\rangle=\sum_\mu\langle f|\mu\rangle\langle\mu|i\rangle e^{iV_\mu}, \tag{5.3}$$

and this is a convergent series.

In what energy region do we expect this eikonal formula to be a good approximation to the true answer? The answer is: when the energy is large, but not *too* large.[17] The set of diagrams we have considered includes interactions between the two extremely energetic particles, but does not include interactions between the pionization products. Another way to say this is that Reggeon number in the t channel is conserved. This means we expect the eikonal to be valid when $g^2\ln s=O(1)$ but $g^2\ln s'\ll 1$, where s' is the subchannel energy between two created particles. Since at Brookhaven and even intersecting storage rings (ISR) energies there is only a small energy dependence in the total cross section, it is reasonable to suppose that $g^2\ln s$ is still small. Thus we can expect that this eikonal form will be valid at the energy ranges of the larger accelerators now being built.

We have verified that the leading T^{2n} terms calculated from the Feynman diagrams agree with those in the eikonal form for elastic scattering (through the tenth order at least), and we believe that it is valid for two particles scattering into n particles. However, it is not correct for processes in which both the initial and final states contain more than two particles. This is because the eikonal describes scattering which takes place in a very short time period compared to the time scale of the particles' self-interaction, for example. Thus, it cannot remain valid for a scattering process which takes place over a long time. Now

consider a scenario in which three particles scatter into three particles. First, two particles come together, interact, and separate. Then, at a *later* time, one of these two particles scatters off the third particle. The correct way to describe such a process is by two eikonals separated by particle propagation.

There are important differences between the eikonal forms in QED and in Yang-Mills theory. In QED, the potential V may be thought of as a generalized static field (elastic and inelastic) due to the target electron, so that e^{iV} is then the amplitude for the scattering of the projectile electron from this potential. Such an interpretation is possible because the target electron remains an electron after the emission of any number of photons. In Yang-Mills theory, however, the target particle carries isospin and its charge state changes as it interacts with the projectile. Thus the concept of a static field no longer applies.

This difference can be seen directly from the diagrammatic calculation. The QED counterpart of the Yang-Mills isospin T is the charge Z of the incident particles. In diagrammatic calculations in QED, the power of Z is always equal to the number of vertices on the high-energy lines. But in Yang-Mills theory the non-Abelian nature of the isospin means that there are many more terms present. For example, the T^2 terms come not only from the one-meson-exchange diagram but from the tower diagrams as well. Physically, these terms represent the effect, mentioned above, of the changing charge state of the target particle.

This explains why in QED, but not in Yang-Mills theory, the potential consists of the lowest-order amplitudes for each process. In particular, in QED the elastic part of the potential represents the exchange of a photon and is related to the Coulomb (or Yukawa) potential between the two high-energy electrons. The counterpart of this term in the Yang-Mills potential is not the exchange of a vector meson, but rather of a Regge pole on which the vector meson lies. Thus, the potential V is a function of the energy of the projectile.

The generalization from boson-boson scattering to fermion-boson or fermion-fermion scattering is trivial. For each fermion replacing a vector meson the space-time factor is multiplied by a factor of $1/2m$, where m is the fermion mass. The generalization to groups other than SU(2) is also simple,[18] since the majority of the isospin manipulations involve only the commutation relation (4.1).

After the results in this paper were obtained, Lo devised a method of generalized leading-term approximation[12] in an attempt to overcome some of the limitations with the present work. His method and results are the main content of his paper published in this issue. His results and ours differ only in nonleading terms. However, the extra terms included in his scheme of approximation leave him with an S matrix which is not explicitly unitary.

ACKNOWLEDGMENTS

Two of us (H.C. and J.D.) wish to thank Professor Ching Ning Yang for the hospitality extended to them during their stay at the Institute of Theoretical Physics at Stony Brook. We are also grateful for many useful discussions with Dr. P. S. Yeung. We acknowledge many discussions with Dr. C. Y. Lo. We also thank him for communicating to us his calculations based on the diagrammatic decomposition of isospin factors. For clarity of presentation, we have also used this method of diagrammatic decomposition to rederive the results originally calculated by the method in Ref. 16. The work of one of us (K.O.) was supported in part by the Norwegian Research Council for Science and Humanities. This work was supported in part by the National Science Foundation under Grant No. PHY-76-12396-A01.

APPENDIX A: TRANSVERSE-MOMENTUM DIAGRAMS

Transverse-momentum diagrams stand for integrals over the transverse momenta. Each diagram consists of a series of vertices arranged vertically connected by line segments. Transverse momentum $\vec{\Delta}_\perp$ flows into the bottom vertex and out of the top vertex; and in between the momentum is conserved at each vertex. The integrals which the diagrams stand for are determined by the following rules:

(i) a factor of $(\vec{q}_\perp^{\,2}+\lambda^2)^{-1}$ for each line segment carrying momentum $\vec{q}_\perp$, unless there is a horizontal bar through that segment, in which case there is no factor,

(ii) $\int d^2\vec{k}_\perp/(2\pi)^2$ for each closed loop, and

(iii) for each horizontal bar through a vertex, a factor of $(\vec{q}_\perp^{\,2}+\lambda^2)$ where $\vec{q}_\perp$ equals the sum of the momentum coming into the vertex from below.

For example, the diagrams representing K_1, $(\vec{\Delta}_{1\perp}^{\,2}+\lambda^2)K_1^2$, and K_3 are shown in Figs. 9(a), 9(b), and 9(c), respectively. K_1 and K_3 are given explicitly by (4.9) and (B10).

APPENDIX B: THE SIXTH-ORDER FEYNMAN-DIAGRAM CALCULATION

In this appendix we give in more detail the calculations of the sixth-order amplitudes from Feynman diagrams.

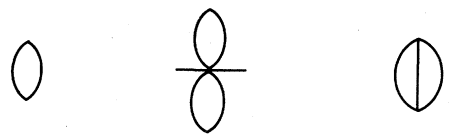

(a) (b) (c)

FIG. 9. Examples of transverse-momentum diagrams which represent the integrals (a) K_1, (b) $(\vec{\Delta}_\perp^2+\lambda^2)K_1^2$, and (c) K_3.

From Table I, the sum of the T^2 terms is

$$(-M_2-M_4-M_{11}-M_{12}-M_{13}-M_{14}+M_{16})\times(\text{the isospin factor represented by Fig. 3}). \tag{B1}$$

From the previous leading-logarithm calculation[5,14] it is known that

$$M_2\sim-\tfrac{1}{2}g^2s\left(\frac{g^2\ln s}{2\pi}\right)^2[2(\vec{\Delta}_\perp^2+\lambda^2)K_1^2+\lambda^2K_1^2-4K_1K_2], \tag{B2}$$

$$M_4\sim\tfrac{1}{2}g^2s\left(\frac{g^2\ln s}{2\pi}\right)^2(\lambda^2K_1^2), \tag{B3}$$

$$M_{11}\sim M_{12}\sim M_{13}\sim M_{14}\sim-\tfrac{1}{2}g^2s\left(\frac{g^2\ln s}{2\pi}\right)^2(K_1K_2), \tag{B4}$$

and

$$M_{16}=O(\ln s), \tag{B5}$$

where

$$K_2=\int\frac{d^2q_\perp}{(2\pi)^2}\frac{1}{\vec{q}_\perp^{\,2}+\lambda^2}. \tag{B6}$$

Thus the space-time part of (B1) equals

$$g^2s\left(\frac{g^2\ln s}{2\pi}\right)^2(\vec{\Delta}_\perp^2+\lambda^2)K_1^2. \tag{B7}$$

Notice that the divergences in the transverse-momentum integrations coming from the integral K_2 cancel out exactly.

Next consider the T^4 terms. From the third column of Table I, one such term is

$$(M_1+M_2-M_{5a}-M_{5b}-M_{6a}-M_{6b}+M_{16}+M_{19}+M_{20})\times[\text{the isospin factor of Fig. 10(a)}]. \tag{B8}$$

We know that[5,11,14]

$$M_1+M_2\sim-\tfrac{1}{2}ig^4s\frac{g^2\ln s}{2\pi}\times[2(\vec{\Delta}_\perp^2+\lambda^2)K_\perp^2+\lambda^2K_1^2-4K_1K_2], \tag{B9a}$$

$$M_{5a}+M_{5b}\sim M_{6a}+M_{6b}\sim ig^4s\frac{g^2\ln s}{2\pi}K_1K_2, \tag{B9b}$$

and

$$M_{16}+M_{19}+M_{20}\sim 2ig^4s\frac{g^2\ln s}{2\pi}K_3, \tag{B9c}$$

where

$$K_3=\int\frac{d^2\vec{q}_{1\perp}}{(2\pi)^2}\frac{d^2\vec{q}_{2\perp}}{(2\pi)^2}\frac{1}{(\vec{q}_{1\perp}^{\,2}+\lambda^2)(\vec{q}_{2\perp}^{\,2}+\lambda^2)[(\vec{\Delta}_\perp-\vec{q}_{1\perp}-\vec{q}_{2\perp})^2+\lambda^2]}. \tag{B10}$$

In deriving (B9c) it is necessary to use (4.16)–(4.19). Separately M_1 and M_2 each contain real terms proportional to $\ln^2 s$ and $\ln s$ but they cancel out in the sum. Further, M_{5a}, M_{5b}, M_{6a}, and M_{6b} each separately contain real terms proportional to $\ln s$, but they too cancel out in the sum. The divergent parts of (B9a) and (B9b) also cancel. Therefore, the space-time part of (B8) equals

$$ig^4s\frac{g^2\ln s}{2\pi}[-(\vec{\Delta}_\perp^2+\lambda^2)K_1^2-\tfrac{1}{2}\lambda^2K_1^2+2K_3]. \tag{B11}$$

The other term proportional to T^4 is, from column two of Table I,

$$(M_3+M_4+M_{5a}+M_{5b}+M_{6a}+M_{6b}+M_7+M_8+M_9+M_{10}+M_{11}+M_{12}+M_{13}+M_{14}-3M_{16}-M_{17}-M_{18}-2M_{19}-2M_{20})\times[\text{the isospin factor of Fig. 6(a)}]. \tag{B12}$$

These amplitudes are given by[5,11,14]

$$M_3+M_4\sim\tfrac{1}{2}ig^4s\frac{g^2\ln s}{2\pi}\lambda^2K_1^2, \tag{B13a}$$

$$M_7+M_{11}\sim M_8+M_{12}\sim M_9+M_{13}\sim M_{10}+M_{14}\sim-\tfrac{1}{2}ig^4s\frac{g^2\ln s}{2\pi}K_1K_2, \tag{B13b}$$

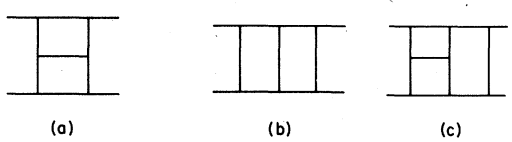

(a) (b) (c)

FIG. 10. Box isospin factors of order (a) T^4 and (b), (c) T^6.

and

$$-3M_{16}-M_{17}-M_{18}-2M_{19}-2M_{20}\sim -2ig^4 s\frac{g^2\ln s}{2\pi}K_3\,. \tag{B13c}$$

Thus the space-time part of (B12) becomes

$$ig^4 s\frac{g^2\ln s}{2\pi}(\tfrac{1}{2}\lambda^2 K_1^2-2K_3)\,. \tag{B14}$$

Again the divergent terms and real $\ln s$ terms cancel out.

Finally, we consider the T^6 terms. From column four of Table I they are

$$(M_{15}+M_{16}+M_{17}+M_{18}+M_{19}+M_{20})\times[\text{the isospin factor of Fig. 10(b)}]. \tag{B15}$$

Using (4.10) through (4.15), we find that the space-time part of (B15) equals

$$-\tfrac{1}{3}g^6 s K_3\,, \tag{B16}$$

which is pure real as expected. This completes the calculation through the sixth order. Note that in the traditional leading-logarithm approximation, the amplitude given by (B15) is dropped. This is the first difference between our present scheme and the traditional leading-logarithm calculation.

If we project these amplitudes into t-channel isospin-exchange channels we find that the T^2 and T^6 terms are predominantly $I=1$ while the T^4 terms are predominantly $I=0$ and $I=2$. For example, if we look at the $I=1$ projection of the T^4 amplitudes given by (4.8), (B11), and (B14), they are in fact of order T^2 and precisely give the imaginary part of the signature factor of the Regge-pole term

$$\frac{g^2}{\vec{\Delta}_\perp^{\,2}+\lambda^2}s^{\alpha_1}(1-e^{-i\pi\alpha_1})(-T_a^{(1)}T_a^{(2)})\,, \tag{B17}$$

where

$$\alpha_1=1-g^2(\vec{\Delta}_\perp^{\,2}+\lambda^2)\frac{1}{2\pi}K_1\,. \tag{B18}$$

APPENDIX C: CALCULATION FROM THE EIKONAL FORMULA

As an illustration of the techniques involved in the calculations from the eikonal formula, we will calculate its $(Tg)^6(g^2\ln s)$ term. Because there is a factor of T^2 from each V, only the $(iV)^3/3!$ term from the power-series expansion of e^{iV} contributes. Besides the g^6 factor associated with the T^6 factor there is an extra g^2 factor which can come either from the Reggeization of one of the exchanged vector mesons or from the creation and subsequent annihilation of a W meson or Z scalar.

Suppose first that one of the exchanged mesons Reggeizes; the isospin factor associated with this process is given in Fig. 10(b), and the space-time amplitude is (see Fig. 11)

$$\begin{aligned}
&2is\left(\frac{-i^3}{3!}\right)\int d^2\vec{b}_\perp e^{i\vec{\Delta}_\perp\cdot\vec{b}_\perp}\langle\vec{p}_{1'},\vec{p}_{2'}\,|\,V^3\,|\vec{p}_1,\vec{p}_2\rangle\\
&\quad=2is\left(\frac{-i^3}{3!}\right)\int d^2\vec{b}_\perp e^{i\vec{\Delta}_\perp\cdot\vec{b}_\perp}\int\frac{d^2\vec{q}_{1\perp}}{(2\pi)^2}e^{-i\vec{q}_{1\perp}\cdot\vec{b}_\perp}\frac{\bar{m}(s,\vec{q}_{1\perp})}{2s}\int\frac{d^2\vec{q}_{2\perp}}{(2\pi)^2}e^{-i\vec{q}_{2\perp}\cdot\vec{b}_\perp}\frac{\bar{m}(s,\vec{q}_{2\perp})}{2s}\int\frac{d^2\vec{q}_{3\perp}}{(2\pi)^2}e^{-i\vec{q}_{3\perp}\cdot\vec{b}_\perp}\frac{\bar{m}(s,\vec{q}_{3\perp})}{2s}\\
&\quad=-\tfrac{1}{3}g^6 s\int\frac{d^2\vec{q}_{1\perp}}{(2\pi)^2}\frac{d^2\vec{q}_{2\perp}}{(2\pi)^2}\frac{d^2\vec{q}_{3\perp}}{(2\pi)^2}(2\pi)^2\delta^{(2)}(\vec{q}_{1\perp}+\vec{q}_{2\perp}+\vec{q}_{3\perp}-\vec{\Delta}_\perp)\frac{1}{(\vec{q}_{1\perp}^{\,2}+\lambda^2)(\vec{q}_{2\perp}^{\,2}+\lambda^2)(\vec{q}_{3\perp}^{\,2}+\lambda^2)}\\
&\qquad\times[1-(1-\alpha(\vec{q}_{1\perp}))\ln s+\cdots][1-(1-\alpha(\vec{q}_{2\perp}))\ln s+\cdots][1-(1-\alpha(\vec{q}_{3\perp}))\ln s+\cdots]\,.
\end{aligned} \tag{C1}$$

Keeping the g^8 terms in (C1) we get

$$g^6 s\frac{g^2\ln s}{2\pi}\int\frac{d^4\vec{q}_{1\perp}}{(2\pi)^2}\frac{d^2\vec{q}_{2\perp}}{(2\pi)^2}\frac{d^2\vec{q}_{3\perp}}{(2\pi)^2}\frac{d^2\vec{q}_{4\perp}}{(2\pi)^2}\frac{(2\pi)^2\delta^{(2)}(\vec{q}_{1\perp}+\vec{q}_{2\perp}+\vec{q}_{3\perp}+\vec{q}_{4\perp}-\vec{\Delta}_\perp)}{(q_{1\perp}^{\,2}+\lambda^2)(q_{2\perp}^{\,2}+\lambda^2)(q_{3\perp}^{\,2}+\lambda^2)(q_{4\perp}^{\,2}+\lambda^2)}\equiv g^6 s\frac{g^2\ln s}{2\pi}K_4\,. \tag{C2}$$

The integral K_4 is represented by the transverse-momentum diagram in Fig. 12(a). Notice that we started

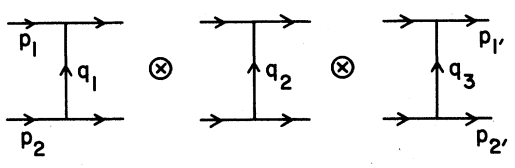

FIG. 11. Schematic representation of a V^3 term calculated from the eikonal formula.

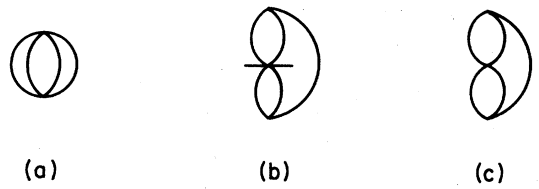

FIG. 12. Transverse-momentum diagrams which appear in the evaluation of the $(Tg)^6(g^2\ln s)$ term. (a) K_4, (b) K_5, (c) K_6.

with a three-Reggeon exchange term (i.e., V^3) and generated a four-meson exchange term by expanding the Reggeized vector-meson propagator. This series expansion

$$\frac{s^{-\alpha(\vec{\Delta}_\perp)}}{\vec{\Delta}_\perp^{\,2}+\lambda^2}=\frac{1}{\vec{\Delta}_\perp^{\,2}+\lambda^2}-\frac{g^2\ln s}{2\pi}\int\frac{d^2\vec{q}_\perp}{(2\pi)^2}\frac{1}{(\vec{q}_\perp^{\,2}+\lambda^2)[(\vec{\Delta}_\perp-\vec{q}_\perp)^2+\lambda^2]}+\cdots \tag{C3}$$

may be expressed diagrammatically in terms of transverse-momentum diagrams, as shown in Fig. 13(a). The elastic part of the three-Reggeon exchange can then be represented as an infinite sum of transverse-momentum diagrams as shown in Fig. 13(b).

Suppose now that a vector meson or scalar is created and then annihilated. There are three ways this can happen, as illustrated in Fig. 14. The amplitude for the process shown in Fig. 14(a) is

$$\begin{aligned}2is\left(\frac{-i^3}{3!}\right)\int d^2b_\perp e^{i\vec{\Delta}_\perp\cdot\vec{b}_\perp}\int\frac{d^2\vec{q}_{1\perp}}{(2\pi)^2}\frac{d^2\vec{q}_{2\perp}}{(2\pi)^2}\frac{d^2\vec{q}_{3\perp}}{(2\pi)^2}\exp(-i\vec{q}_{1\perp}\cdot\vec{b}_\perp-i\vec{q}_{2\perp}\cdot\vec{b}_\perp-i\vec{q}_{3\perp}\cdot\vec{b}_\perp)\\ \times\left(\frac{g^3}{\sqrt{2E}}\right)^2 g^2\int\frac{d^2k_\perp}{(2\pi)^2}\int_{-\omega}^{\omega}\frac{dk_3}{2\pi}\frac{1}{(\vec{q}_{1\perp}^{\,2}+\lambda^2)[(\vec{q}_{1\perp}^{\,2}-\vec{k}_\perp)^2+\lambda^2](\vec{q}_{2\perp}^{\,2}+\lambda^2)[(\vec{q}_{2\perp}^{\,2}+\vec{k}_\perp)^2+\lambda^2](\vec{q}_{3\perp}^{\,2}+\lambda^2)}\\ \times\left(\sum_{i=1}^{3}\Gamma(q_1,q_1-k)\cdot\epsilon^i(k)\Gamma(q_2,q_2+k)\cdot\epsilon^i(k)I_1+\lambda^2 I_2\right),\end{aligned} \tag{C4}$$

where $E=(k_3^2+\vec{k}_\perp^{\,2}+\lambda^2)^{1/2}$ is the energy of the created particle, where the sum in i ($i=1,2,3$) is over the three independent polarization vectors $\epsilon^i(k)$, where only the g^8 term has been kept (so that $s_i^{\alpha(\vec{\Delta}_{i\perp})-1}$ has been set equal to unity), and where I_1 and I_2 are isospin factors which are represented diagrammatically by the diagrams in Figs. 10(c) and 10(b), respectively.

We make an aside to calculate the product of the vertex factors for the vector mesons,

$$\begin{aligned}\sum_{i=1}^{3}\Gamma_1(\Delta_1,\Delta_2)\cdot\epsilon^i(k)\Gamma_2(\Delta_1',\Delta_2')\cdot\epsilon^i(k)&=\sum_{i=1}^{3}\Gamma_{1\mu}\Gamma_{2\nu}\epsilon_\mu^i\epsilon_\nu^i\\ &=\Gamma_{1\mu}\Gamma_{2\nu}\left(-g_{\mu\nu}+\frac{k_\mu k_\nu}{\lambda^2}\right)=-\Gamma_1\cdot\Gamma_2=-\tfrac{1}{2}\Gamma_{1+}\Gamma_{2-}-\tfrac{1}{2}\Gamma_{1-}\Gamma_{2+}+\Gamma_{1\perp}\cdot\Gamma_{2\perp},\end{aligned} \tag{C5}$$

where we have used the property of the vertex function, $\Gamma\cdot k=0$. This equals

$$\begin{aligned}&-\tfrac{1}{2}(2k_+)\left(\frac{1}{2}-\frac{\vec{\Delta}_{1\perp}^{\,2}+\lambda^2}{\vec{k}_\perp^{\,2}+\lambda^2}\right)(-2k_-)\left(\frac{1}{2}-\frac{\vec{\Delta}_{2'\perp}^{\,2}+\lambda^2}{\vec{k}_\perp^{\,2}+\lambda^2}\right)-\tfrac{1}{2}(-2k_-)\left(\frac{1}{2}-\frac{\vec{\Delta}_{2\perp}^{\,2}+\lambda^2}{\vec{k}_\perp^{\,2}+\lambda^2}\right)(2k_+)\left(\frac{1}{2}-\frac{\vec{\Delta}_{1'\perp}^{\,2}+\lambda^2}{\vec{k}_\perp^{\,2}+\lambda^2}\right)-(\vec{\Delta}_{1\perp}+\vec{\Delta}_{2\perp})\cdot(\vec{\Delta}_{1'\perp}+\vec{\Delta}_{2'\perp})\\ &\quad=2(\vec{k}_\perp^{\,2}+\lambda^2)\left[\left(\frac{1}{2}-\frac{\vec{\Delta}_{1\perp}^{\,2}+\lambda^2}{\vec{k}_\perp^{\,2}+\lambda^2}\right)\left(\frac{1}{2}-\frac{\vec{\Delta}_{2'\perp}^{\,2}+\lambda^2}{\vec{k}_\perp^{\,2}+\lambda^2}\right)+\left(\frac{1}{2}-\frac{\vec{\Delta}_{1'\perp}^{\,2}+\lambda^2}{\vec{k}_\perp^{\,2}+\lambda^2}\right)\left(\frac{1}{2}-\frac{\vec{\Delta}_{2\perp}^{\,2}+\lambda^2}{\vec{k}_\perp^{\,2}+\lambda^2}\right)\right]\\ &\qquad+(\vec{\Delta}_{1\perp}^{\,2}+\lambda^2)+(\vec{\Delta}_{2\perp}^{\,2}+\lambda^2)+(\vec{\Delta}_{1'\perp}^{\,2}+\lambda^2)+(\vec{\Delta}_{2'\perp}^{\,2}+\lambda^2)-(\vec{k}_\perp^{\,2}+\lambda^2)-2[(\vec{\Delta}_{1\perp}+\vec{\Delta}_{1'\perp})^2+\lambda^2]-\lambda^2\\ &\quad=2\frac{(\vec{\Delta}_{1\perp}^{\,2}+\lambda^2)(\vec{\Delta}_{2'\perp}^{\,2}+\lambda^2)+(\vec{\Delta}_{1'\perp}^{\,2}+\lambda^2)(\vec{\Delta}_{2\perp}^{\,2}+\lambda^2)}{\vec{k}_\perp^{\,2}+\lambda^2}-2[(\vec{\Delta}_{1\perp}+\vec{\Delta}_{1'\perp})^2+\lambda^2]-\lambda^2.\end{aligned} \tag{C6}$$

The only dependence on the longitudinal momentum k_3 in (C4) is therefore through E, and

$$\int_{-\omega}^{\omega}\frac{dk_3}{2\pi}\frac{1}{2E}\sim\int_{1/2\omega}^{2\omega}\frac{dk_-}{2\pi}\frac{1}{2k_-}=\frac{1}{2}\frac{\ln s}{2\pi}. \tag{C7}$$

Therefore, the amplitude in (C4) becomes

$$-\tfrac{1}{6}g^6 s\,\frac{g^2\ln s}{2\pi}\left[(4K_4-2K_5-\lambda^2K_6)I_1+\lambda^2K_6I_2\right], \tag{C8}$$

where

$$K_5=\int\frac{d^2\vec{q}_{1\perp}}{(2\pi)^2}\frac{d^2\vec{q}_{2\perp}}{(2\pi)^2}\frac{d^2\vec{q}_{3\perp}}{(2\pi)^2}\frac{(\vec{q}_{1\perp}+\vec{q}_{2\perp})^2+\lambda^2}{(\vec{q}_{1\perp}^{\,2}+\lambda^2)(\vec{q}_{2\perp}^{\,2}+\lambda^2)(\vec{q}_{3\perp}^{\,2}+\lambda^2)[(\vec{q}_{1\perp}+\vec{q}_{2\perp}-\vec{q}_{3\perp})^2+\lambda^2][(\vec{\Delta}_\perp-\vec{q}_{1\perp}-\vec{q}_{2\perp})^2+\lambda^2]} \tag{C9a}$$

and

$$K_6=\int\frac{d^2\vec{q}_{1\perp}}{(2\pi)^2}\frac{d^2\vec{q}_{2\perp}}{(2\pi)^2}\frac{d^2\vec{q}_{3\perp}}{(2\pi)^2}\frac{1}{(\vec{q}_{1\perp}^{\,2}+\lambda^2)(\vec{q}_{2\perp}^{\,2}+\lambda^2)(\vec{q}_{3\perp}^{\,2}+\lambda^2)[(\vec{q}_{1\perp}+\vec{q}_{2\perp}-\vec{q}_{3\perp})^2+\lambda^2][(\vec{\Delta}_\perp-\vec{q}_{1\perp}-\vec{q}_{2\perp})^2+\lambda^2]}. \tag{C9b}$$

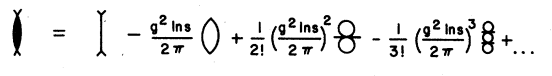

(a)

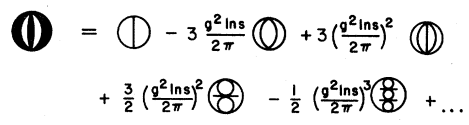

(b)

FIG. 13. (a) The expansion of the Reggeized propagator in terms of transverse-momentum diagrams. (b) The expansion of the elastic part of the three-Reggeon exchange amplitude.

The transverse-momentum diagrams corresponding to K_5 and K_6 are given in Figs. 12(b) and 12(c), respectively. The amplitudes for the processes shown in Figs. 14(b) and 14(c) are also given by (C8), with the isospin factors appropriately adjusted.

Equation (C6), which represents the product of two vertex functions, can formally be represented in terms of transverse-momentum diagrams as illustrated in Fig. 15. In that figure, slashes on a line mean that the corresponding propagator is absent and the two vertices at either end of the line are to be fused together into one. An example is given in Fig. 16.

From the above example, it should be clear that the following rules apply when calculating the terms proportional to T^{2n} via the eikonal formula.

(i) There is an overall factor of $i^{n-1}/n!$.

(ii) There is a single factor of $2s$ from (3.3) and

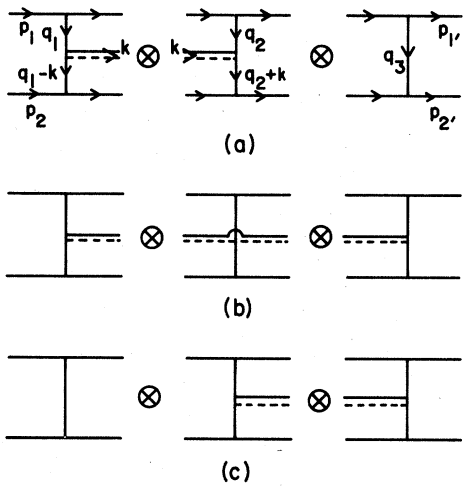

FIG. 14. The three ways in which to generate, from the eikonal formula, a term of the order $(Tg)^6(g^2 \ln s)$ if a particle is created and then destroyed. The double line stands for either a vector meson or a scalar.

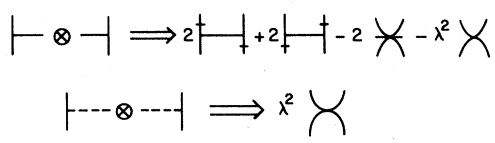

FIG. 15. A schematic representation of the product of two three-vector-meson vertices.

n factors of $1/[2(\Pi_m f_m)^{1/2}]$ from (3.4) where the products are over the incoming and outgoing particles in the appropriate initial, final, or intermediate states; and there is a factor of $2s$ from each of the n potentials. The net result is a factor of $2s/\Pi_i(2E_i)$ where the product is over all intermediate-state particles which are created and then destroyed.

(iii) These energy factors are integrated over the longitudinal momenta to give a factor of

$$g^2\int_{-\omega}^{\omega}\frac{dk_3}{2\pi}\frac{1}{2E}\sim g^2\int_{1/2\omega}^{2\omega}\frac{dk_-}{(2\pi)(2k_-)}=\frac{1}{2}\left(\frac{g^2\ln s}{2\pi}\right).$$

If the minus momenta are ordered there will be additional factors, as the 1/2! in

$$g^2\int_{1/2\omega}^{2\omega}\frac{dk_{1-}}{2\pi}\frac{1}{2k_{1-}}g^2\int_{1/2\omega}^{k_{1-}}\frac{dk_{2-}}{2\pi}\frac{1}{2k_{2-}}=\frac{1}{2!}\left(\frac{g^2}{2}\frac{\ln s}{(2\pi)}\right)^2.$$

(iv) There is a factor of $1/(\vec{l}_\perp^{\,2}+\lambda^2)$ for each of the exchanged mesons in a potential V, and an integration $\int d^2\vec{k}_\perp/(2\pi)^2$ over the transverse momenta of each closed loop.

(v) From the Reggeization of a vector meson there are factors of $-g^2\ln s/2\pi$ times the appropriate transverse-momentum integration (see Fig. 13).

(vi) The squares of the vertex factors are given in Fig. 15.

The results of the calculation from exponentiation through the tenth order are given in Table III. They agree with the results of the Feynman-diagram calculation as claimed.

APPENDIX D

Here we present a simple model[19] in one space and one time dimension in which the perturbation

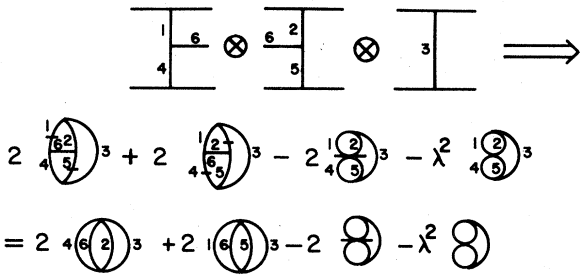

FIG. 16. An example of the use of the identity of Fig. 15.

series for the eikonal diverges. There is no isospin in this model and the vertex factor in the numerator is just a constant, but the propagators are Reggeized. For simplicity we take $g=\lambda=1$. The scattering amplitude $\mathfrak{M}$ is given by

$$\mathfrak{M}=2is(1-e^{iV}). \tag{D1}$$

The matrix elements of the potential V for a process in which n particles (with energies E_i, $i=1,2,\ldots,n$) are created or destroyed is

$$s^{-\alpha}\frac{1}{\left[\prod_{i=1}^{n}(2E_i)\right]^{1/2}}. \tag{D2}$$

Here α is a constant since there is no transverse dimension. Then the elastic matrix element of $\mathfrak{M}$ is (see the rules for generating the scattering amplitude from the eikonal, given at the end of Appendix C)

$$2s\sum_{m=1}^{\infty}\frac{i^{m-1}}{m!}s^{-m\alpha}\sum_{n=0}^{\infty}\binom{m}{2}^{n}\frac{[\ln s/2(2\pi)]^n}{n!}$$

$$=2s\sum_{m=1}^{\infty}\frac{i^{m-1}}{m!}s^{[m(m-1)/8\pi]-m\alpha}, \tag{D3}$$

which diverges if $s>1$.

---

*Permanent address: Department of Mathematics, Massachusetts Institute of Technology, Cambridge, Massachusetts 02139.

[1]H. Cheng, J. Dickinson, C. Y. Lo, K. Olaussen, and P. S. Yeung, Phys. Lett. 76B, 129 (1978).

[2]H. Cheng, invited talk in the Proceedings of the International Meeting on the Frontiers of Physics, Singapore, 1978 (unpublished).

[3]H. Cheng and T. T. Wu, Phys. Rev. Lett. 24, 1456 (1970) and references quoted therein.

[4]V. S. Fadin, E. A. Kuraev, and L. N. Lipatov, Phys. Lett. 60B, 50 (1975).

[5]H. Cheng and C. Y. Lo, Phys. Rev. D 15, 2959 (1977).

[6]J. A. Dickinson, Phys. Rev. D 16, 1863 (1977).

[7]This can be seen by denoting the charge of the high-energy incident particles in QED by Ze, while keeping the charge of all other electrons to be e. Then Z in QED is the counterpart of T in Yang-Mills theories. In QED, an amplitude is proportional to Z^{2n} if it corresponds to a diagram with $2n$ vertices on the two lines representing the particles of charge Z. Among these diagrams of Z^{2n}, our scheme in QED singles out precisely the ones which give the leading terms.

[8]It may appear that the difficulty with our approximation scheme is that T for a physical particle is of the order of unity, hence Tg cannot be of the order of unity if g^2 is small. However, if g^2 is small and $g^2\ln s$ is of the order of unity, then all the terms we drop are small no matter whether Tg is small or of the order of unity. The main difficulty with our scheme is that terms larger than the Froissart bound have been dropped. Therefore, no matter what the size of Tg is, this scheme cannot be rigorously justified. In Yang-Mills theories, the diagrams with n vertices on the two lines of isospin T do not necessarily contribute to the T^n terms. An example is given in Fig. 5. Thus we must calculate all diagrams to extract these leading terms.

[9]G. Molière, Z. Naturforsch. 2, 133 (1947).

[10]R. J. Glauber, in *Lectures in Theoretical Physics*, edited by W. E. Brittin *et al.* (Wiley-Interscience, New York, 1959), Vol. 1.

[11]J. A. Dickinson, Ph.D. thesis, Massachusetts Institute of Technology (unpublished).

[12]C. Y. Lo, preceding paper, Phys. Rev. D 23, 508 (1981).

[13]For references on these graphical methods, see R. Penrose, in *Combinatorial Mathematics and Its Application*, edited by D. J. A. Welsh (Academic, New York, 1971), pp. 221–244; E. El-Baz and B. Castel, *Graphical Methods of Spin Algebras* (Dekkar, New York, 1972); G. P. Canning, Phys. Rev. D 8, 1151 (1973); G. P. Canning, Niels Bohr Inst. Report No. NBI-HE-24-2, 1974 (unpublished); G. P. Canning, Phys. Rev. D 12, 2505 (1975); P. S. Yeung, *ibid.* 13, 2306 (1976); R. F. Cahalan and D. Knight, *ibid.* 14, 2126 (1976); P. Cvitanovic, *ibid.* 14, 1536 (1976); J. Mandula, MIT course notes (unpublished).

[14]B. McCoy and T. T. Wu, Phys. Rev. D 12, 3257 (1975); 13, 1076 (1976); L. Tyburski, *ibid.* 13, 1107 (1976); H. T. Nieh and Y.-P. Yao, *ibid.* 13, 1082 (1976); L. N. Lipatov, Yad. Fiz. 23, 642 (1976) [Sov. J. Nucl. Phys. 23, 338 (1976)]; L. L. Frankfurt and V. E. Sherman, Yad. Fiz. 23, 1099 (1976) [Sov. J. Nucl. Phys. 23, 581 (1976); A. L. Mason, Nucl. Phys. B117, 493 (1976).

[15]H. Cheng and T. T. Wu, Phys. Rev. 186, 1611 (1969).

[16]H. Cheng, J. Dickinson, C. Y. Lo, and K. Olaussen, Lett. Nuovo Cimento 25, 175 (1979).

[17]For more details, see Ref. 2.

[18]P. Yeung, Phys. Rev. D 13, 2306 (1976). See also L. Tyburski in Ref. 4.

[19]Similar models have been considered by S. Auerbach, R. Aviv, R. Sugar, and R. Blankenbecler, Phys. Rev. D 6, 2216 (1972), and by R. Blankenbecler and H. M. Fried, *ibid.* 8, 678 (1973).